Electronic Supplementary Material (ESI) for RSC Advances.

Supplementary Information:

Performance enhancement in ZnO nanowire based double Shottky-Barriers photodetector by applying optimized Ag nanoparticles

Xin Zhao[a,b], Fei Wang[a,*], Linlin Shi[a,b], Yunpeng Wang[a], Haifeng Zhao[a], Dongxu Zhao[a,*]

[a]*State key laboratory of luminescence and applications, Changchun Institute of Optics, Fine Mechanics and Physics, Chinese Academy of Sciences, 3888 Dongnanhu Road, Changchun 130021, People's Republic of China*

[b]*University of the Chinese Academy of Sciences, Beijing 100049, People's Republic of China*

E-mail: wangf@ciomp.ac.cn, zhaodx@ciomp.ac.cn

Experiment methods

1. ZnO nanowire synthesis.

Finely grinded high purity ZnO nanopowder (Aldrich, 99.99%) and graphite powder (Aldrich, < 20 micron) with the 1:1 weight ratio were mixed together and then transferred into an alumina boat. After that, a substrate was located face down above the source materials with the distance of 5 mm. For achieving a better aligned nanowire array, we chose Si (100) wafer with ZnO seed layer deposited by ALD method as the production collecting substrate. The alumina boat loaded with ZnO/C mixture and Si substrate was transferred into the middle of the furnace tube. The synthesis process was performed as following steps: First, the furnace tube was purged with Ar (99.999%) flow at 200 sccm for 10 min to reach the 1 atm inert ambient before the furnace start to heat. Second, the temperature inside the tube was elevated to 900 ℃ at a rate of 50 ℃/min with a constant Ar stream rate of 100 sccm, then kept the temperature for 40 min. Finally, the furnance was cooled to room temperature, then the dark gray or white product could be observed on the seed layer.

2. Device fabrication.

According to the previous reports, there must be adequate nanowire appearing in the gap between two electrodes to achieve efficient assembly. Based on this consideration, we chose the proper nanowire concentration in ethanol solution. The NWs on substrate of 5×5 mm^2 were exfoliated by gently, short time ultrasonic pulse for 15 s to form a 0.5 ml stable NWs solution. After dispensing 5 μl of the dispersed NWs solution onto the counter electrodes, a sinusoidal potential (1 MHz, 20 Vpp) was applied on the electrodes for approximately 20 s through an arbitrary function generator. The AC electric field signal was monitored by a oscilloscope during the fabrication process. The finished device here needed no further treatment.

3. Characterization of the Nanocomposites.

The structural quality of synthesized ZnO nanowire was investigated by X-ray diffraction (XRD) (Bruker AXS D8 FOCUS, Cu$K\alpha$ radiation at room temperature). The data was acquired under the scanning speed of 2.4 ^{o}/min at the operating voltage of 40 kV. The detailed XRD pattern of ZnO nanowire is shown in the Fig. S1. The inset is the top view of the ZnO nanowire on Si substrate. The product related XRD pattern contains three peaks correspond to the (100), (002) and (101) planes, respectively, which indicates the ZnO nanowire have good quality with wurtzite crystal structure. And the strong intensity of peak to (002) plane compared to others presented that the ZnO nanowire prefer the growth orientation along [002] c-axis direction.

X-ray photoelectron spectroscopy (XPS) analysis was carried out for further investigation of the chemical composition and states of the ZnO/Ag heterostructure with a Thermo ESCALAB 250 instrument using monochromatic Al$K\alpha$ X-ray source in the constant-pass energy mode. The binding energy regions including O1s, Zn2p and Ag3d were scanned and C1s peak (284.6 eV) was used as the standard to calibrated the Bonding energy level. Fig. S2 contains the survey of ZnO/Ag heterostructure XPS spectrum, as well as the corresponding spectra of Zn2p, O1s and Ag3d. It should be noted that the sample here was decorated using Ag nanoparticle of about 15nm in diameter. The survey scan spectrum of Zn, O, Ag and C is shown and labelled in Fig. S2(a). It is clear that no peaks belong to other elements, which indicating a good purity of synthesized samples. In the Fig. S2(b), there are two symmetrical peaks located at 1044.46 eV and 1021.3 eV, corresponding to the $Zn2p_{1/2}$ and $Zn2p_{3/2}$, respectively. The spin-orbit coupling induced Zn2p states splitting is about 23 eV and the locations of the two binding energies are shifted to lower energy region due to the decorated Ag NPs. All the hints above show that the Zn atom exist in the sample in the form of Zn^{2+} states. The asymmetrical O1s spectrum could be fitted with two adjacent gauss peaks in the Fig. S2(c), one at high binding energy of 531.44 eV, feature signal of hydroxyl groups absorption, and a low binding energy at 530.01 eV associated with oxygen ions in the crystal lattice. Fig. S2(d) shows that the

XPS spectrum of the Ag3d binding energy levels are located at 373.53 eV and 367.5 eV, respectively. The splitting of $Ag3d_{3/2}$ and $Ag3d_{5/2}$ peaks is about 6 eV that confirmed the Ag NPs were mainly in the metallic state.

The regional energy dispersive X-ray spectroscopy (EDX) analysis, EDX line-scan and energy-loss electron spectroscopy (EELS) chemical mapping of the ZnO/Ag heterostructure were performed using transmission electron microscopy (TEM, Tecnai G^2 F20 S-TWIN). A typical EDX spectrum of ZnO nanowire decorated with ~10 nm Ag NPs is given in the Fig. S3. Highlight area of the inset picture demonstrates the selected area to acquire the EDX spectrum. The EDX spectrum peaks corresponding to the Zn, O, and Ag elements are clearly visible, which further confirms that the proper chemical composition of the nanomaterials. EDX line-scan profiles and ELLS chemical mappings of the synthesized ZnO/Ag-NPs composites in selected positions are shown in Fig. S4 and Fig. S5, respectively.

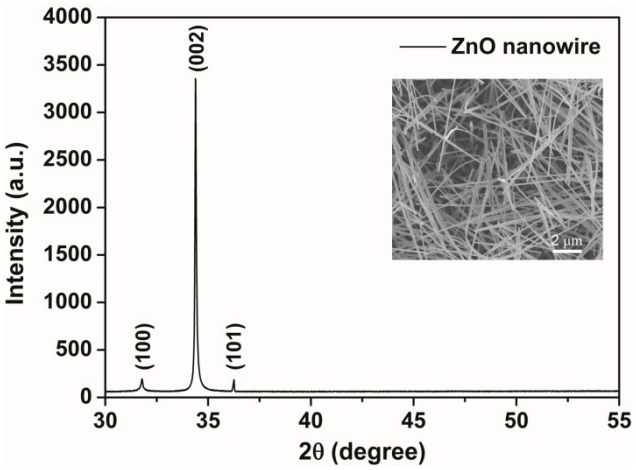

Fig. S1 XRD pattern of as-synthesized ZnO nanowires on a silicon (100) substrate. The inset shows the SEM image of the grown nanwires.

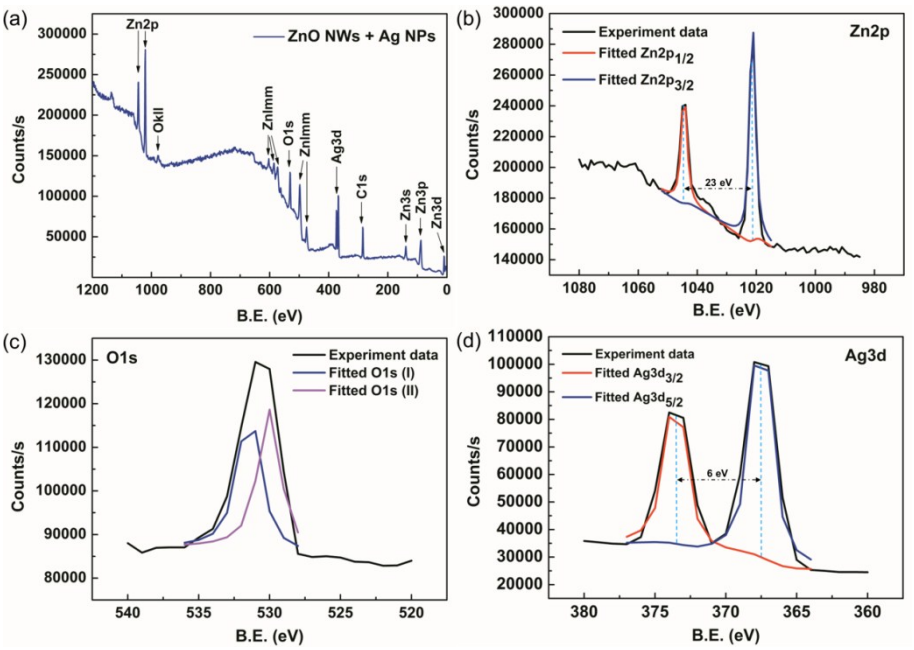

Fig. S2 XPS spectra of the ZnO nanowires decorated with ~15nm Ag NPs. (a) The survey XPS spectrum. The regional XPS spectrums of (b) Zn2p, (c) O1s and (d) Ag 3d.

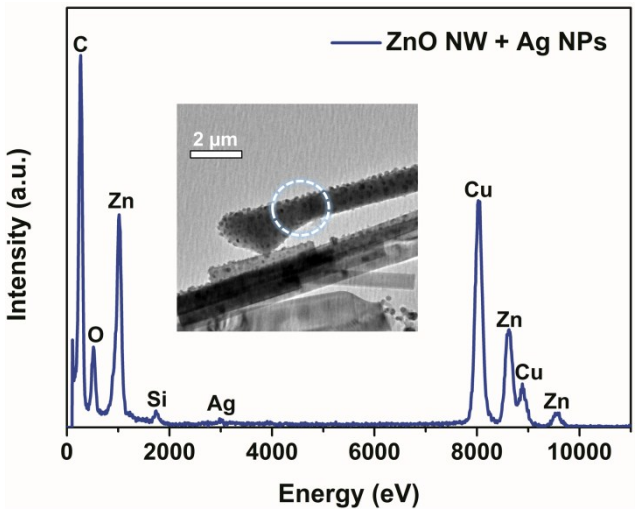

Fig. S3 EDX spectrum of the ZnO/Ag-NPs heterostructure from the selected area. The inset shows the bright-field TEM image of the synthesized composite.

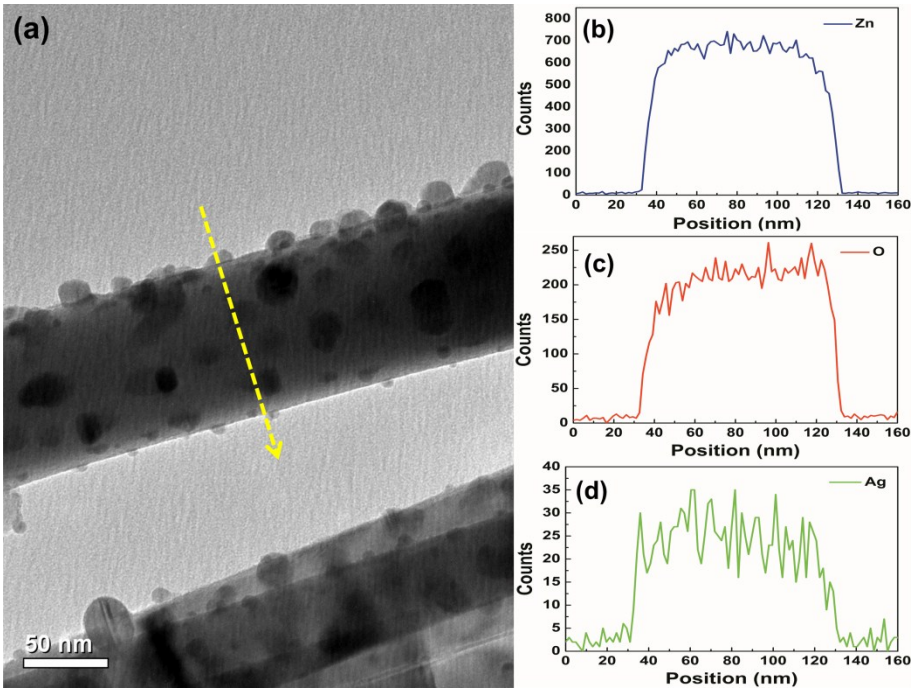

Fig. S4 TEM image and energy dispersive X-ray (EDX) line-scan profiles of the ZnO/Ag-NPs. (a) low- magnification TEM image of a single ZnO nanowire with ~10 nm Ag NPs, (b)-(d) show the EDX line-scan profiles corresponding to Zn, O and Ag element along the radial direction of a nanowire as shown in (a) with a yellow arrow.

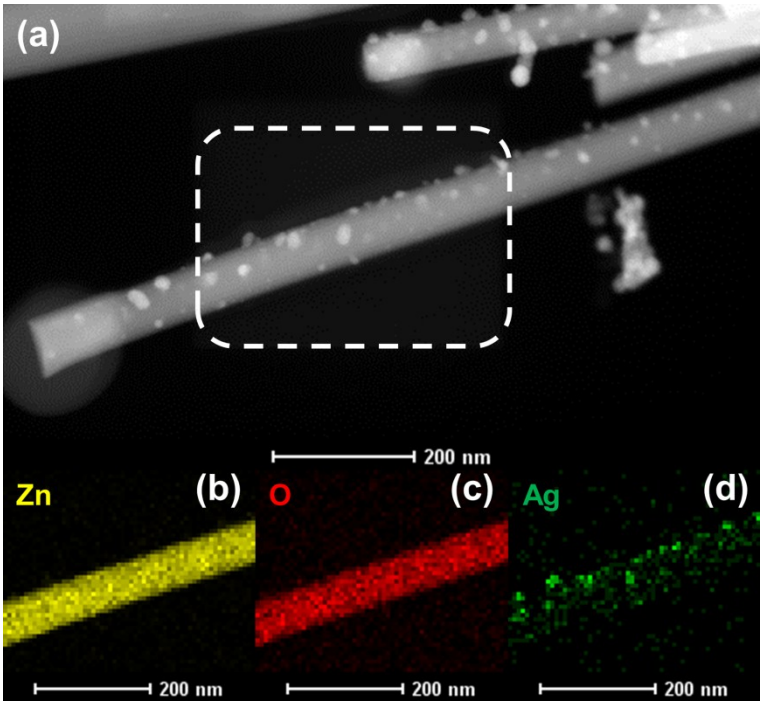

Fig. S5 STEM image and EELS chemical mappings of the ZnO/Ag-NPs. (a) presents the high-angle annular dark-field (Z-contrast) scanning transmission electron microscopy (HAADF-STEM) image of a single ZnO nanowire decorated with Ag NPs. (b)-(d) illustrate elemental mappings of Zn, O and Ag in the selected area in (a).